ORIGINAL ARTICLE

The potential of eggshell hydroxyapatite, collagen, and EGCG (HAp-Col-EGCG) scaffold as a pulp regeneration material

Elline Elline [a,b], **Kun Ismiyatin** [c,*], **Theresia Indah Budhy** [d], **Anuj Bhardwaj** [e,f]

[a] *Student of Doctoral Program, Faculty of Dental Medicine, Universitas Airlangga, Indonesia*
[b] *Department of Conservative Dentistry, Universitas Trisakti, Kyai Tapa Grogol No 26, Jakarta, Indonesia*
[c] *Department of Conservative Dentistry, Faculty of Dental Medicine. Universitas Airlangga, Indonesia*
[d] *Department of Oral and Maxillofacial Pathology, Faculty of Dental Medicine. Universitas Airlangga, Indonesia*
[e] *Department of Conservative Dentistry, Faculty of Dental Medicine. Universitas Airlangga, Indonesia*
[f] *Department of Conservative Dentistry and Endodontics, College of Dental Sciences and Hospital, Rau, Indore, India*

Abstract *Background:* Hydrogel scaffold is a biomaterial that can facilitate cells in forming a tissue structure. It can promote cell adhesion, migration, and proliferation. Further research to find a new scaffold from natural resources is challenging, so this study aimed to characterize a hydrogel composite scaffold, which has the potential to be used as a regenerative material.

Methods: The formulation of HAp-Col-EGCG was mixed with different ratios of 1%, 2%, and 4% hydroxyapatite. We analyzed its injectability, pH, and gelation time. Scanning electron microscopy (SEM), energy X-ray Spectroscopy (EDX), and Fourier-transform infrared spectroscopy (FTIR) were used to evaluate the surface morphologies, element composition, and chemical properties of HAp-Col-EGCG.

Results: The results showed that the injectability test was almost 90 % in all groups. There was no significant difference in the median value of the pH at 0, 20, and 60 min in all groups, but there was a significant difference at 40 min. The average gelation times in all groups were not significant. SEM-EDX showed a microporous scaffold, with the HAp particles well distributed in the collagen pores at a ratio of 1.9, 2.29, and 1.89 Ca/P. The FTIR results showed intermolecular bonds in the

* Corresponding authors at: Department of Conservative Dentistry, Airlangga University, 60132 Surabaya, Indonesia (K. Ismiyatin)
E-mail addresses: elline@trisakti.ac.id (E. Elline), kun-is@fkg.unair.ac.id (K. Ismiyatin), theresia-i-b-s@fkg.unair.ac.id (T. Indah Budhy), dranuj_84@yahoo.co.in (A. Bhardwaj).
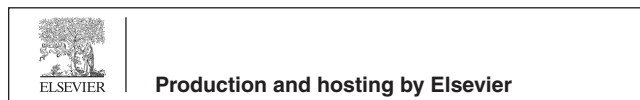
HAp-Col-EGCG scaffold. The X-ray diffraction analysis showed that collagen and EGCG did not affect the crystal structure and size of HAp. Cytotoxicity test showed more dental pulp cell viability at the 4 % HAp concentration at 514.35 ± 15.45.

Conclusion: This study indicates that hydrogel scaffold from eggshell hydroxyapatite, collagen, and EGCG has a high potential for pulp regenerative therapy.

1. Introduction

Nowadays, regenerative treatment approaches in developing pulp dentin complex repair involve using mesenchymal stem cells, growth factors, and a scaffold (Khurshid et al., 2022; Paduano et al., 2016). The scaffold can provide a framework for the cell homing process. It should be biocompatible, simple application in the dentin, injectable, non-toxic, biodegradable, and solidified at 37 °C. Based on several criteria, a hydrogel scaffold can be considered to develop (Abbass et al., 2020; Chang et al., 2017; Raucci et al., 2018). Scaffolds from natural sources can be obtained from eggshell hydroxyapatite, bovine collagen type I with epigallocatechin-3-gallate modification. Hydroxyapatite is a material with a similar composition to bone and teeth, and eggshell is a popular one (Ahmadian et al., 2019; Elline and Ismiyatin, 2021; Khandelwal and Prakash, 2016). An eggshell nanohydroxyapatite scaffold has interconnected pores, contains high levels of calcium carbonate that induces the differentiation of dental pulp cells (Afriani, 2015; Okamoto et al., 2020; Sancilio et al., 2018).

Collagen is a material that can penetrate intermolecularly and forms a gel, so it is suitable for use in rigid dentin composition (Kwon et al., 2017). Hydroxyapatite and collagen are humans' leading natural components of tissues and proteins and can be synthesized using the sol–gel method (Sathiyavimal et al., 2020; Yu et al., 2020). Nanohydroxyapatite can be distributed between collagen fibers, and EGCG addition can create a smooth surface, stimulating bone regeneration (Permatasari and Yusuf, 2019). Crosslinked EGCG has been beneficial as an anti-inflammation agent (Kwon et al., 2017). In this research, a hydrogel scaffold was formulated from eggshell hydroxyapatite, collagen, and EGCG to benefit each material (HAp-Col-EGCG). This study aimed to prove that HAp-Col-EGCG composite has the potential to be used as a scaffold for pulp regeneration material.

2. Materials and methods

2.1. Fabrication of HAp-Col-EGCG hydrogel

The preparation of the material was done using eggshell nanohydroxyapatite (Pertiwi Technology, Bogor, Indonesia), 5 mg/mL collagen I bovine (Gibco, Thermofisher Scientific, USA), and EGCG (Sigma Aldrich, E4268, ≥80 %, USA). Hydroxyapatite was dissolved in deionized water at a concentration of 1 %, 2 %, and 4 % and stirred for one h at 350 rpm (Permatasari and Yusuf, 2019). Then, ten μmol/L of EGCG was added to the hydroxyapatite solution and stirred until homogenous at a cold temperature (Kwon et al., 2017). 3 mg/mL collagen solution was prepared by adding phosphate-buffered saline (Gibco, Thermofisher Scientific,

USA), sodium hydroxide, and distilled water (Merck Millipore Mili-Q) (Gibco, Thermofisher, 2014). The collagen solution was mixed with hydroxyapatite and the EGCG solution at a cold temperature for 30 min. After that, 2 % hydroxypropyl methylcellulose (HPMC) (Benecel, K100M, Ashland, Wilmington, USA) was added until homogenous and colloidal at room temperature. The mixing process was performed at Biocore laboratory (Universitas Trisakti, Indonesia) and several characterization were obtained from LIPI Fisika (Serpong, Tangerang, Indonesia).

2.2. Injectability test

The characteristic of the flow was determined through a 10 cc, 21G syringe (Terumo Corporation, Tokyo, Japan) with 64.1 N maximal force (1 ml/10 s) (Gutierrez and Munakomi, 2022; Sharma et al., 2016). The mass before injection and mass extruded from the syringe were weighed. The percentage of injectability was using the following formula: % injectability = (*mass extruded from the syringe/total mass before injection*) × 100 %, and the procedure was repeated three times (Hikmawati et al., 2019; Takallu et al., 2019).

2.3. Gelation time and pH

Gelation time was measured by the inverted tube method (De Mori et al., 2019). The process was determined by the color changes to an opaque color. The optimal gelation time is 5 to 30 min, providing enough time for application with a stable gel formulation (Bendtsen and Wei, 2017). Three replications were done to get the average value. The pH value was measured using a pH-meter (PHS- 3E, INESA Instrument, Shanghai, China) and repeated three times for 1 h; right after mixing, 20, 40, and 60 min at room temperature (Yan et al., 2016).

2.4. Microporosity of HAp-Col-EGCG hydrogel scaffold

The morphology of the HAp-Col-EGCG scaffold was analyzed using SEM-EDX (Hitachi S4700, Tokyo, Japan). Before the SEM imaging, HAp-Col-EGCG hydrogels were freeze-dried at − 80 °C for 24 h. The freeze-dried samples were coated with an Au layer, and we measured the largest and smallest pore diameters (Mulyawan et al., 2022; Podhorská et al., 2020).

2.5. Fourier-transform infrared spectroscopy (FT-IR)

The functional group of the HAp-Col-EGCG formulation was analyzed using FTIR (Thermo Fisher Scientific Nicolet iS-10, USA). Samples of HAp-Col-EGCG with 1 %, 2 %, and 4 %

HAp were investigated at the 400–4,000 cm^{-1} wavenumber range (Mulyawan et al., 2022).

2.6. X-ray diffraction (XRD) analysis

The XRD pattern was analyzed by XRD (Smartlab Rigaku, Tokyo, Japan) using copper (Cu) as the X-ray source, with a voltage of 40 kV and current of 40 mA, at a range of 2θ from 10° to 90° scan rate of 5° min^{-1}. It can determine the microstructure characteristics such as compound phase composition and crystallinity using the Bragg–Bentano scan method.

2.7. Cytotoxicity test

Human dental pulp stem cells (hDPSCs) obtained from PT Prodia Stem Cell, Indonesia. Cytotoxicity test of was done by the 3-(4,5- dimethyl-2-thiazolyl)-2.5-diphenyl-2H-tetrazolium bromide (MTT) assay. The cell viability information was known by the change of formazan salt due to mitochondrial activation of living cells. An enzyme-linked immunosorbent assay reader was to analyze the optical density of the formazan salt. The percentage of cell viability formula using a relative optical density. The material of the samples is not toxic if the cell viability is > 50 % (ISO 10993–5) (Hikmawati et al., 2019; Srisomboon et al., 2022).

$$Relative\ OD = \frac{OD\ of\ test\ group}{OD\ of\ control} \times 100$$

2.8. Statistical analysis

Shapiro–Wilk normality test was carried out on all data obtained. If the data was normal, one-way analysis of variance (ANOVA) was used. Otherwise, the data was analyzed using Kruskal–Wallis. Data are described as the mean and standard deviation value or its median at $P < 0.05$. Statistics were performed using SPSS 25 (SPSS Inc, Chicago, IL, USA).

3. Results

3.1. Injectability test

According to the injectability test, samples with 1 %, 2 %, and 4 % HAp can be injected (Fig. 1 and Table 1). One-way ANOVA showed no significant difference between all groups ($P > 0.05$).

3.2. Gelation time test

The average gelation time was shown in Fig. 2 and Table 1. Fig. 2 A,B show the HAp-Col-EGCG before and after the gelation process. All samples fulfilled the criteria that should be 5 – 30 min.[23] The concentration of 1 %, 2 %, and 4 % HAp showed no significant difference in gelation time ($P > 0.05$).

3.3. pH value

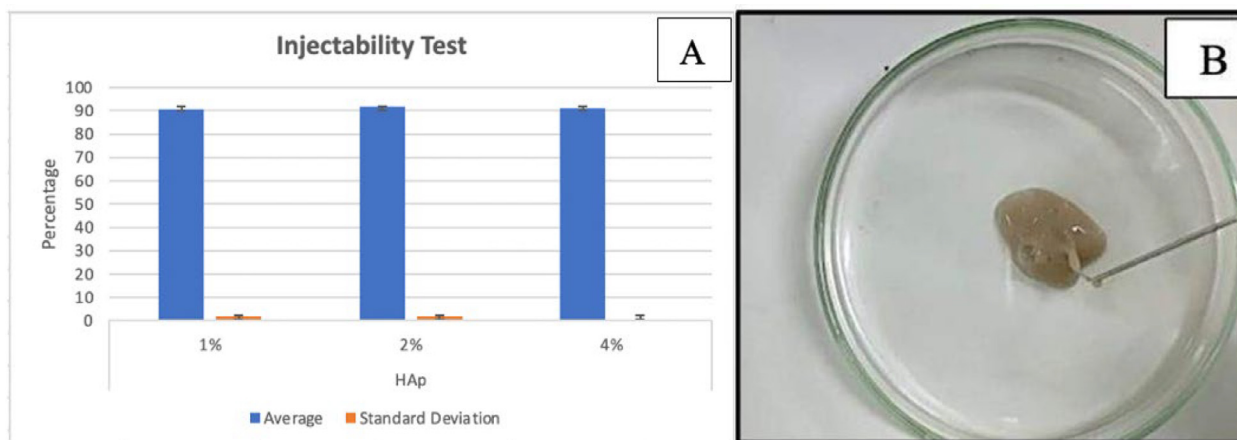Data were not normally distributed. The results showed significant differences in the pH value at 0, 20, and 60 min

Fig. 1 Graph the injectability test results of HAp-Col-EGCG (A) and injected through the 21-G syringe (B).

Table 1 The statistical result of scaffolds' injectability test and gelation times.

Scaffold HAp-Col-EGCG	Mean ± SD			p
	1 %	2 %	4 %	
Injectibility (%)	90.4 ± 1.93	92.13 ± 1.97	91.06 ± 0.75	0.477
Gelation times (s)	326 ± 23.3	366 ± 9.16	342.33 ± 12.5	0.06

*One-way ANOVA (p > 0.05).
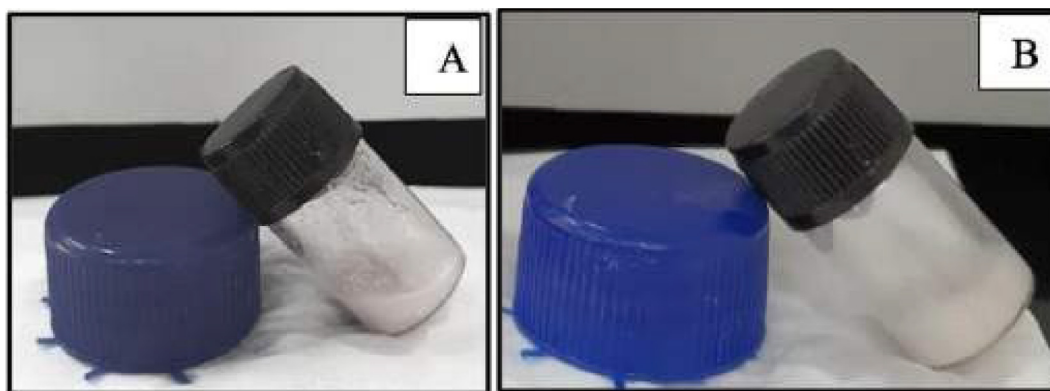
Fig. 2   HAp-Col-EGCG formulation before (A) and after (B) gelation.

Table 2   Comparison of the pH scaffold formulation at different times.

pH				
	Time			
Scaffold	0	20	40	60
	Med (min- max)	Med (min- max)	Med (min- max)	Med (min- max)
1:1	7.98 (7.75– 8.11)	7.82 (7.82– 8.12)	7.98 (7.81–8.11)	8.12 (7.82–8.12)
1:2	7.34 (7.32–7.45)	7.32 (7.32–7.51)	7.98 (7.98–8.11)	8.46 (8.3–8.63)
1:4	9.18 (9.17–9.19)	9.26 (9.26–9.28)	9.26 (9.22–9.35)	9.31 (9.3–9.34)
p	0.027*	0.025*	0.057	0.027*

*Friedmann ($P < 0.05$); *Kruskal–Wallis ($P < 0.05$).

($P < 0.05$). This result showed that pH values are higher at a higher HAp concentration (Table 2).

3.4. Functional group test (FTIR)

The FTIR result showed in Fig. 3. The hydroxyl group in HAp were seen at 3,416.1 cm^{-1} to 3,431.49 cm^{-1}, respectively, which are related to O─H stretching and confirmed the presence of hydrogen bond in Hap (Fern and Salimi, 2021). The major PO$_4$ groups peaks were obtained at 1022–1023 cm^{-1}, due to asymmetric stretching of the phosphate group. The HAp functional groups were OH$^-$ and PO$_4^{3-}$, so they were identified as Hap (Fern and Salimi, 2021; Rogina et al., 2019; Siswanto et al., 2020).

The amide I and EGCG were identified, by a wavenumber at 1,651.94 cm^{-1} to 1,653.44 cm^{-1}, with medium N─H bending and strong stretching of C═O.[29] Amide II was found at 1,560.71 cm^{-1} to 1,561.20 cm^{-1} wavenumbers. In amide III, peak absorbance was shown with medium C─N stretching at 1,022.20 cm^{-1} to 1,198.98 cm^{-1}(Vishwakarma et al., 2015). The absorbance at 2,929.38 and 2,927.94 were the stretching of C–CH3, which is specific to the HPMC functional group (Fig. 3) (Hikmawati et al., 2019).

3.5. Xrd analysis

The XRD pattern in all the sample groups showed an identical pattern. The 2θ, characterization with angles of 31.48°, 31.65°,

and 31.73°, respectively. It could be concluded that collagen and EGCG did not affect the crystal structure of HAp.

All samples formed a hexagonal crystal structure, but there were difference in crystal size value, 11.4745 nm (1 % HAp), 19.8254 nm (2 % HAp), and 18.1769 nm (4 % HAp). The 1 % HAp concentration resulted in a smaller crystal size and the larger crystal size was found in 2 % HAp concentration.

3.6. Microporosity and EDS analysis of Hap-Col-EGCG hydrogel scaffold

Data were not normal distributed, and they showed no significant difference in the scaffold pore diameter in all samples ($P > 0.05$). The diameter porous (μm) data were performed in median (min–max) value; 21.1 (7.84–44.61) (1 % HAp); 27.19 (8.11–76.71) (2 %HAp); 21.55 (4.96–132.17) (4 % HAp) (p > 0.05). The pores in these concentrations could support cell attachment, growth, and proliferation and have the potential for dentin pulp regeneration treatment (Panseri et al., 2016; Vishwakarma et al., 2015). Agglomerated HAp was also dispersed in the porous collagen (Fig. 4.A–C).

EDS analysis of the Ca, P, and O composition proved HAp presence. It showed a homogenous distribution of elements in the synthesis. The Ca/P ratio of 1.9, 2.29, and 1.89. The value of Ca/P approaching the natural extracellular matrix from the mineral phase is 1.67 (EzEldeen et al., 2021). All Ca/P ratios of the samples were above the stochiometric value (1.67); thus, the synthesis of the scaffold modified the ratio of Ca/P from
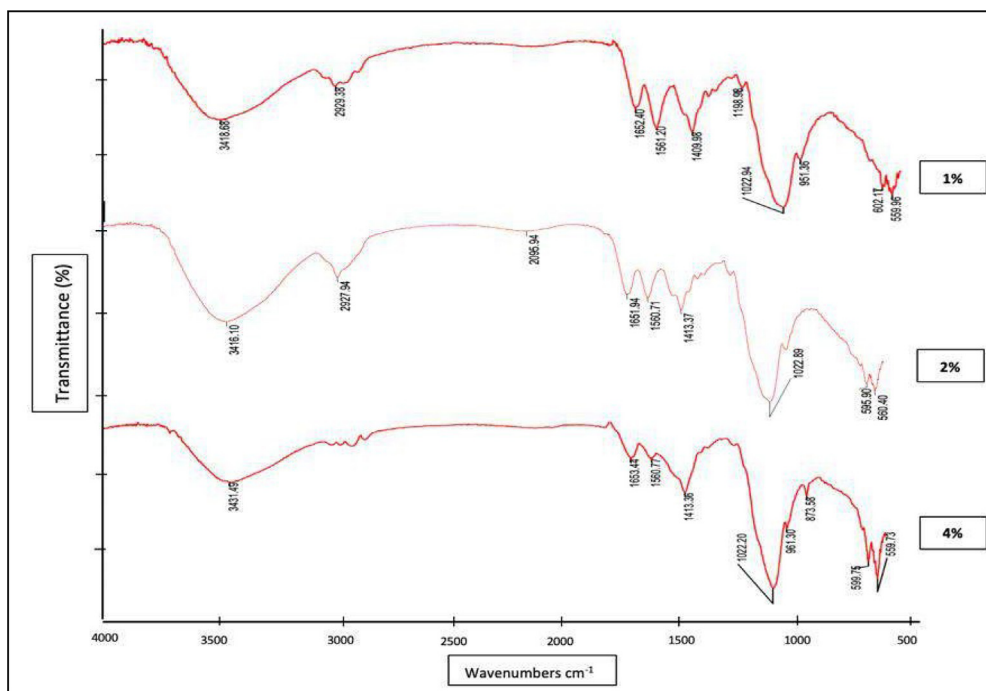
Fig. 3 Spectra of the HAp-Col-EGCG, with three variations in HAp concentration.

Fig. 4 HAp-Col-EGCG scaffold with 1% (A), 2% (B), and 4% (C) showed interconnected pores and agglomerated HAp dispersed in a the scaffold.

stochiometric. The HAp-Col-EGCG scaffold with 4 % HAp was closest to 1.67.

3.7. Cytotoxicity test

This test was performed for 24 h, and it proved that the HAp-Col-EGCG scaffold was non-toxic because the viability of the cells was above 50 %. The results were 158.388 ± 10.484 (1 % HAp); 240.638 ± 10.469 (2 % HAp); 330.016 ± 14.963 (4 % HAp). It showed significant differences in the dental pulp cell viability for each group of scaffolds ($P < 0.05$).

4. Discussion

The results of this study showed that HAp-Col-EGCG can be formed into a hydrogel scaffold. An injectable form hydrogel can improve the biological stability of the biomaterial and is

affected by the sample's syringe diameter, viscosity, and solvent (Ren et al., 2018). Suspension agent (2 % HPMC) can increase the viscosity and stability of the formula (Charlena et al., 2020). HPMC does not affect the chemical analysis and biological reaction (Ciolacu et al., 2020; Ghadermazi et al., 2019). Injectable application in the dental pulp region is essential because the dental pulp is in a rigid and limited area Hikmawati et al., 2019).

The inverted test tube method was used to perform a gelation time test of the HAp-Col- EGCG scaffold at 37 °C. Too fast gelation would not make enough time for clinical application, whereas slow gelation time would make it difficult to target the application area (Ren et al., 2018). The recommended gelation time is 5 to 30 min, and all group samples had an ideal gelation time.

The latest literature has reported that the initial pH is crucial in determining the morphology and size of the formulation structure, whether sphere, roller, needle, etc. The pH can indi-

cate supersaturation that can influence the ion balance. If there are increases or decreases in the OH^- composition, these will affect and modify the concentrations of Ca^{2+}, $PO4^{3-}$, and $(HPO4)^{2-}$ ions. The agglomerate nanoparticles in the SEM analysis decreased particle size when the pH value decreased (López-Ortiz et al., 2020). In the present study, the pH value had a hexagonal phase, with a stable pH value in each group.

According to Okamoto et al. (2020), cell death was found in DPC cultures at a pH of 3.5 to 5.5. It showed cell growth or arrest at a pH of 6.5 to 7.5 and showed mild proliferation at a pH of 9.5 (Hirose et al., 2016). In this study, the HAp-Col-EGCG scaffold with 4 % HAp had a pH value approaching 9.5. It can be used to support regeneration in the inflamed pulp (Hirose et al., 2016).

The FTIR results identified that the functional group indicates O─H stretching, which confirmed eggshell HAp, EGCG, and HPMC, similar to the results of Rogina et al., that indicated hydrogel composite at 3,150–3,600 cm^{-1} wavenumbers (Rogina et al., 2019). The evidence of strong PO_4^{3-} groups which confirmed HAp was 1040 cm^{-1} and 1090 cm^{-1} (Hooi et al., 2021) but following the study of Siswanto et al. (2020), $PO4^{3-}$ was also identified the bending of PO_4^{3-} at 500 cm^{-1} to 630 cm^{-1} that also proved of HAp existance, it supports this study that had phosphate bending at 559.96 cm^{-1} to 602.17 cm^{-1}.

In this study, the amide I, II, and III peaks were stable for all samples, indicating that the triple helix structure of collagen is still intact and maintained with the addition of EGCG or Hap (Permatasari and Yusuf, 2019). Similar to Hikmawati et al. (2019), HPMC-specific group function was also identified, indicating that HPMC also formed a hydrogen bond.

The possible HAp-Col-EGCG bond is a hydrogen bond which take place between a collagen hydrogen atom and oxygen in HAp. It creates mineralized collagen between collagen structure and the crystal in HAp, which showed from C═O band (Siswanto et al., 2020). Another study also discovered that the bonding mechanism started with Ca^{2+} ions from HAp interacting with amide I ($NH2$) in collagen (Susanto et al., 2019).

The crystal structure of HAp did not change because of collagen and EGCG addition. A hexagonal structure with the $P63/m$ space group is still formed. The 1 %, 2 %, and 4 % HAp crystal size result supports previous studies that crystal length and width averages of 21 ± 9 nm and 6 ± 1.5 nm. The main peak of HAp in HAp-Col-EGCG formulation was identified at a range that is similar to a previous study which identified HAp at 2θ of 31.7°, 32.2°, and 32.9° (In et al., 2020). The XRD result showed that the number of crystal sizes would decrease when the pH value is low (López-Ortiz et al., 2020). It was found that the particle size increases when the pH value increases from 6 to 13 (Chithra et al., 2015).

In this study, the nanoparticle crystal size was also larger when the scaffold pH value increased in 4 % HAp. Increasing H^+ can create the favorable formation of monoclinic HAp. Decreasing the OH^- concentration can cause solution saturation reduction, so when the pH decreases, the nucleation and growth of crystals reduce (López-Ortiz et al., 2020).

The median diameter pore of HAp-Col-EGCG scaffold from all groups could support cell attachment, growth, and proliferation. All Ca/P ratio of the samples was above the stochiometric (1.67), and the HAp-Col-EGCG scaffold with 4 % HAp was the nearest to 1.67. The higher Ca/P ratio presents

due to higher HAp concentration, it indicated the existence of B-type carbonate phosphate which identical with a mineral in human bones that promotes cell adhesion (Hooi et al., 2021). Higher Ca/P ratio will support the smaller particle size so the degradation in the living body facilitated so the Ca and P component will absorb faster. It can induced bone repair (Zhang et al., 2019).

The modified scaffolds have micropores about 1 μm to 100 μm in size (Iga et al., 2020). Scaffold with a microtubular size (20 μm) is similar to the structure of dentin, and it can support gel proliferation and differentiation of odontoblast cells (Haeri et al., 2017). Microporosity can increase the biomaterial surface area and increased protein adsorption will further increase cell adhesion (Herda and Puspitasari, 2018). It can support the transportation of nutrients and the bone regeneration process (Sobczak-Kupiec et al., 2021).

The combination of HAp or collagen with several flavonoids can support human osteoblast-like cell proliferation and differentiation, and regenerating bone structure. EGCG contains flavonoid can support the proliferation of seeding cells in sponges (Sobczak-Kupiec et al., 2021). In the present study, The percentage of living cell after HAp-Col-EGCG scaffold application was high. All samples support dental pulp cell proliferation. The higher HAp concentration is related to the higher viability of hDPSCs. Several characteristics have not been studied, so the researcher should explore other formula characteristics, such as antibacterial effect or bioactive formula release. Thus, this confirmed the potential of the HAp-Col-EGCG scaffold.

5. Conclusion

The HAp-Col-EGCG fulfilled several ideal hydrogel scaffold criteria. The composition of the scaffold with 4 % HAp concentration indicates the closest to the stoichiometric value. The FTIR analysis showed covalent bonds in all samples. The collagen was not denatured with HAp and EGCG addition. This material is non-toxic and highly likely to be used as a pulp regeneration induction material. In this study, not all the physical characterization tests were performed. Other characterizations such as antibacterial activity, the release of the bioactive material, and the clinical trial in the animal model should be performed.

Declaration of Competing Interest

The authors declare that they have no known competing financial interests or personal relationships that could have appeared to influence the work reported in this paper.

References

Abbass, M.M.S., El-Rashidy, A.A., Sadek, K.M., Moshy, S.E., Radwan, I.A., Rady, D., Dörfer, C.E., Fawzy El-Sayed, K.M., 2020. Hydrogels and dentin-pulp complex regeneration: From the

benchtop to clinical translation. Polymers 12, 2935. https://doi.org/10.3390/polym12122935.

Afriani, F., 2015. Perancah berpori hidroksiapatit dan B-tricalcium phosphate dari limbah cangkang telur ayam dengan porogen alginat [Porous scaffold of hydroxyapatite and -tricalcium phosphate from chicken egg shell waste with porogen alginate] (Master thesis). IPB University, Bogor.

Ahmadian, E., Eftekhari, A., Dizaj, S.M., Sharifi, S., Mokhtarpour, M., Nasibova, A.N., Khalilov, R., Samiei, M., 2019. The effect of hyaluronic acid hydrogels on dental pulp stem cells behavior. Int. J. Biol. Macromol. 140, 245–254. https://doi.org/10.1016/j.ijbiomac.2019.08.119.

Bendtsen, S.T., Wei, M., 2017. In vitro evaluation of 3D bioprinted tripolymer network scaffolds for bone tissue regeneration. J. Biomed. Mater. Res. A 105, 3262–3272. https://doi.org/10.1002/jbm.a.36184.

Chang, B., Ahuja, N., Ma, C., Liu, X., 2017. Injectable scaffolds: Preparation and application in dental and craniofacial regeneration. Mater. Sci. Eng. R Rep. 111, 1–26. https://doi.org/10.1016/j.mser.2016.11.001.

Charlena, U., M.F., Wati, A.K.,, 2020. Addition of hydroxypropyl methylcellulose to hydroxyapatite-chitosan composite as an injectable bone substitute. AIP Conf. Proc. 2243,. https://doi.org/10.1063/5.0004043 030004.

Chithra, M.J., Sathya, M., Pushpanathan, K., 2015. Effect of pH on crystal size and photoluminescence property of ZnO nanoparticles prepared by chemical precipitation method. Acta Metall. Sin. Engl. Lett. 28, 394–404. https://doi.org/10.1007/s40195-015-0218-8.

Ciolacu, D.E., Nicu, R., Ciolacu, F., 2020. Cellulose-based hydrogels as sustained drug-delivery systems. Materials (Basel) 13, 5270. https://doi.org/10.3390/ma13225270.

De Mori, A., Hafidh, M., Mele, N., Yusuf, R., Cerri, G., Gavini, E., Tozzi, G., Barbu, E., Conconi, M., Draheim, R.R., Roldo, M., 2019. Sustained release from injectable composite gels loaded with silver nanowires designed to combat bacterial resistance in bone regeneration applications. Pharmaceutics 11, 116. https://doi.org/10.3390/pharmaceutics11030116.

Elline, E., Ismiyatin, K., 2021. Nanohydroxiapatite using chicken eggshell waste and its characterization. Malays. J. Med. Health Sci. 17, 83–86.

EzEldeen, M., Loos, J., Mousavi Nejad, Z., Cristaldi, M., Murgia, D., Braem, A., Jacobs, R., 2021. 3D-printing-assisted fabrication of chitosan scaffolds from different sources and cross-linkers for dental tissue engineering. Eur. Cell. Mater. 41, 485–501 https://doi.org/10.22203/eCM.v041a31.

Fern, H.W., Salimi, M.N., 2021. Hydroxyapatite nanoparticles produced by direct precipitation method: Optimization and characterization studies. In: Presented at the Proceedings of Green Design and Manufacture 2020, p. 020215. https://doi.org/10.1063/5.0044252.

Ghadermazi, R., Hamdipour, S., Sadeghi, K., Ghadermazi, R., Khosrowshahi Asl, A., 2019. Effect of various additives on the properties of the films and coatings derived from hydroxypropyl methylcellulose—A review. Food Sci. Nutr. 7, 3363–3377. https://doi.org/10.1002/fsn3.1206.

Gibco, Thermofisher, 2014. Collagen I, Bovine [WWW Document]. URL https://assets.fishersci.com/TFS-Assets/LSG/manuals/A1064401_Bovine_collagen_I_PI.pdf.

Gutierrez, J.J.P., Munakomi, S., 2022. Intramuscular Injection, in: StatPearls. StatPearls Publishing, Treasure Island (FL).

Haeri, M., Sagomonyants, K., Mina, M., Kuhn, L.T., Goldberg, A.J., 2017. Enhanced differentiation of dental pulp cells cultured on microtubular polymer scaffolds in vitro. Regen. Eng. Transl. Med. 3, 94–105. https://doi.org/10.1007/s40883-017-0033-z.

Herda, E., Puspitasari, D., 2018. Tinjauan peran dan sifat material yang digunakan sebagai scaffold dalam rekayasa jaringan [Overview of the role and properties of materials used as scaffolds in tissue engineering]. J. Mater. Kedokt. Gigi 5, 56–63.

Hikmawati, D., Maulida, H.N., Putra, A.P., Budiatin, A.S., Syahrom, A., 2019. Synthesis and characterization of nanohydroxyapatite-gelatin composite with streptomycin as antituberculosis injectable bone substitute. Int. J. Biomater. 2019, 7179243. https://doi.org/10.1155/2019/7179243.

Hirose, Y., Yamaguchi, M., Kawabata, S., Murakami, M., Nakashima, M., Gotoh, M., Yamamoto, T., 2016. Effects of extracellular pH on dental pulp cells in vitro. J. Endod. 42, 735–741. https://doi.org/10.1016/j.joen.2016.01.019.

Hooi, M.T., Phang, S.W., Yow, H.Y., David, E., Kim, N.X., Choo, H.L., 2021. FTIR spectroscopy characterization and critical comparison of poly(vinyl)alcohol and natural hydroxyapatite derived from fish bone composite for bone-scaffold. J. Phys. Conf. Ser. 2120,. https://doi.org/10.1088/1742-6596/2120/1/012004 012004.

Iga, C., Paweł, S., Marcin, Ł., Justyna, K.-L., 2020. Polyurethane composite scaffolds modified with the mixture of gelatin and hydroxyapatite characterized by improved calcium deposition. Polymers 12, 410. https://doi.org/10.3390/polym12020410.

In, Y., Amornkitbamrung, U., Hong, M.-H., Shin, H., 2020. On the crystallization of hydroxyapatite under hydrothermal conditions: Role of sebacic acid as an additive. ACS Omega 5, 27204–27210. https://doi.org/10.1021/acsomega.0c03297.

Khandelwal, H., Prakash, S., 2016. Synthesis and characterization of hydroxyapatite powder by eggshell. J. Miner. Mater. Charact. Eng. 4, 119–126. https://doi.org/10.4236/jmmce.2016.42011.

Khurshid, Z., Alnaim, A.J.A., Alhashim, A.A.A., Imran, E., Adanir, N., 2022. Future of decellularized dental pulp matrix in regenerative endodontics. Eur. J. Dent. https://doi.org/10.1055/s-0041-1741012.

Kwon, Y.-S., Kim, H.-J., Hwang, Y.-C., Rosa, V., Yu, M.-K., Min, K.-S., 2017. Effects of epigallocatechin gallate, an antibacterial cross-linking agent, on proliferation and differentiation of human dental pulp cells cultured in collagen scaffolds. J. Endod. 43, 289–296. https://doi.org/10.1016/j.joen.2016.10.017.

López-Ortiz, S., Mendoza-Anaya, D., Sánchez-Campos, D., Fernandez-García, M.E., Salinas-Rodríguez, E., Reyes-Valderrama, M.I., Rodríguez-Lugo, V., 2020. The pH effect on the growth of hexagonal and monoclinic hydroxyapatite synthesized by the hydrothermal method. J. Nanomater. 2020, 5912592. https://doi.org/10.1155/2020/5912592.

Mulyawan, I., Danudiningrat, C.P., Soesilawati, P., Aulanni'am, A., Yuliati, A., Suroto, H., Bramantoro, T., Rizqiawan, A., Moon, S.-Y., 2022. The characteristics of demineralized dentin material sponge as guided bone regeneration based on the FTIR and SEM-EDX tests. Eur. J. Dent. https://doi.org/10.1055/s-0042-1743147.

Okamoto, M., Matsumoto, S., Sugiyama, A., Kanie, K., Watanabe, M., Huang, H., Ali, M., Ito, Y., Miura, J., Hirose, Y., Uto, K., Ebara, M., Kato, R., Yamawaki-Ogata, A., Narita, Y., Kawabata, S., Takahashi, Y., Hayashi, M., 2020. Performance of a biodegradable composite with hydroxyapatite as a scaffold in pulp tissue repair. Polymers 12, 937. https://doi.org/10.3390/polym12040937.

Paduano, F., Marrelli, M., White, L.J., Shakesheff, K.M., Tatullo, M., 2016. Odontogenic differentiation of human dental pulp stem cells on hydrogel scaffolds derived from decellularized bone extracellular matrix and collagen type I. PloS One 11, 0148225. https://doi.org/10.1371/journal.pone.0148225.

Panseri, S., Montesi, M., Dozio, S.M., Savini, E., Tampieri, A., Sandri, M., 2016. Biomimetic scaffold with aligned microporosity designed for dentin regeneration. Front. Bioeng. Biotechnol. 4, 48. https://doi.org/10.3389/fbioe.2016.00048.

Permatasari, H.A., Yusuf, Y., 2019. characteristics of carbonated Hydroxyapatite Based on Abalone Mussel Shells (Halioitis asinina) synthesized by precipitation method with aging time variations. IOP Conf. Ser. Mater. Sci. Eng. 546,. https://doi.org/10.1088/1757-899X/546/4/042031 042031.

Podhorská, B., Vetrík, M., Chylíková-Krumbholcová, E., Kománková, L., Banafshehvaragh, N.R., Šlouf, M., Dušková-Smrčková, M., Janoušková, O., 2020. Revealing the true morphological

structure of macroporous soft hydrogels for tissue engineering. Appl. Sci. 10, 6672. https://doi.org/10.3390/app10196672.

Raucci, M.G., Demitri, C., Soriente, A., Fasolino, I., Sannino, A., Ambrosio, L., 2018. Gelatin/nano-hydroxyapatite hydrogel scaffold prepared by sol-gel technology as filler to repair bone defects. J. Biomed. Mater. Res. A 106, 2007–2019. https://doi.org/10.1002/jbm.a.36395.

Ren, B., Chen, X., Du, S., Ma, Y., Chen, H., Yuan, G., Li, J., Xiong, D., Tan, H., Ling, Z., Chen, Y., Hu, X., Niu, X., 2018. Injectable polysaccharide hydrogel embedded with hydroxyapatite and calcium carbonate for drug delivery and bone tissue engineering. Int. J. Biol. Macromol. 118, 1257–1266. https://doi.org/10.1016/j.ijbiomac.2018.06.200.

Rogina, A., Sandrk, N., Teruel-Biosca, L., Antunovic, M., Ivankovic, M., Ferrer, G.G., 2019. Bone-mimicking injectable gelatine/hydroxyapatite hydrogels. Chem. Biochem. Eng. Q. 33, 325–336.

Sancilio, S., Gallorini, M., Di Nisio, C., Marsich, E., Di Pietro, R., Schweikl, H., Cataldi, A., 2018. Alginate/hydroxyapatite-based nanocomposite scaffolds for bone tissue engineering improve dental pulp biomineralization and differentiation. Stem Cells Int. 2018, 9643721. https://doi.org/10.1155/2018/9643721.

Sathiyavimal, S., Vasantharaj, S., LewisOscar, F., Selvaraj, R., Brindhadevi, K., Pugazhendhi, A., 2020. Natural organic and inorganic–hydroxyapatite biopolymer composite for biomedical applications. Prog. Org. Coat. 147,. https://doi.org/10.1016/j.porgcoat.2020.105858 105858.

Sharma, A., Patel, C., Mandlik, J., 2016. Comparative evaluation of two remineralizing agents in limiting dental erosion. IP Indian J. Conserv. Endod. 1, 86–92.

Siswanto, S., Hikmawati, D., Kulsum, U., Rudyardjo, D.I., Apsari, R., Aminatun, A., 2020. Biocompatibility and osteoconductivity of scaffold porous composite collagen–hydroxyapatite based coral for bone regeneration. Open Chem. 18, 584–590. https://doi.org/10.1515/chem-2020-0080.

Sobczak-Kupiec, A., Drabczyk, A., Florkiewicz, W., Głąb, M., Kudłacik-Kramarczyk, S., Słota, D., Tomala, A., Tyliszczak, B., 2021. Review of the applications of biomedical compositions containing hydroxyapatite and collagen modified by bioactive components. Materials (Basel) 14, 2096. https://doi.org/10.3390/ma14092096.

Srisomboon, S., Kettratad, M., Stray, A., Pakawanit, P., Rojviriya, C., Patntirapong, S., Panpisut, P., 2022. Effects of silver diamine nitrate and silver diamine fluoride on dentin remineralization and cytotoxicity to dental pulp cells: An in vitro study. J. Funct. Biomater. 13, 16. https://doi.org/10.3390/jfb13010016.

Susanto, A., Satari, M.H., Abbas, B., Koesoemowidodo, R.S.A., Cahyanto, A., 2019. Fabrication and characterization of chitosan-collagen membrane from barramundi (Lates calcarifer) scales for guided tissue regeneration. Eur. J. Dent. 13, 370–375. https://doi.org/10.1055/s-0039-1698610.

Takallu, S., Mirzaei, E., Azadi, A., Karimizade, A., Tavakol, S., 2019. Plate-shape carbonated hydroxyapatite/collagen nanocomposite hydrogel via in situ mineralization of hydroxyapatite concurrent with gelation of collagen at pH = 7.4 and 37°C. J. Biomed. Mater. Res. B Appl. Biomater. 107, 1920–1929. https://doi.org/10.1002/jbm.b.34284.

Vishwakarma, A., Sharpe, P., Shi, S., Ramalingam, M., 2015. Stem Cell Biology and Tissue Engineering in Dental Sciences. Elsevier, Philadelphia, PA.

Yan, J., Miao, Y., Tan, H., Zhou, T., Ling, Z., Chen, Y., Xing, X., Hu, X., 2016. Injectable alginate/hydroxyapatite gel scaffold combined with gelatin microspheres for drug delivery and bone tissue engineering. Mater. Sci. Eng. C Mater. Biol. Appl. 63, 274–284. https://doi.org/10.1016/j.msec.2016.02.071.

Yu, L., Rowe, D.W., Perera, I.P., Zhang, J., Suib, S.L., Xin, X., Wei, M., 2020. Intrafibrillar mineralized collagen–hydroxyapatite-based scaffolds for bone regeneration. ACS Appl. Mater. Interfaces 12, 18235–18249. https://doi.org/10.1021/acsami.0c00275.

Zhang, Y., Shao, H., Lin, T., Peng, J., Wang, A., Zhang, Z., Wang, L., Liu, S., Yu, X., 2019. Effect of Ca/P ratios on porous calcium phosphate salt bioceramic scaffolds for bone engineering by 3D gel-printing method. Ceram. Int. 45, 20493–20500. https://doi.org/10.1016/j.ceramint.2019.07.028.